



A New Class of HIV-1 Protease Inhibitor: The Crystallographic Structure, Inhibition and Chemical Synthesis of an Aminimide Peptide Isostere

Earl E. Rutenber,^a Fiona McPhee,^b Alan P. Kaplan,^c Steven L. Gallion,^c Joseph C. Hogan, Jr.,^c
Charles S. Craik^{a,b,*} and Robert M. Stroud^{a,b}

^aDepartment of Biochemistry and Biophysics, ^bDepartment of Pharmaceutical Chemistry, University of California at San Francisco, San Francisco, CA 94143 U.S.A.

^cArQule, Inc., Medford, MA 02155 U.S.A.

Abstract—The essential role of HIV-1 protease (HIV-1 PR) in the viral life cycle makes it an attractive target for the development of substrate-based inhibitors that may find efficacy as anti-AIDS drugs. However, resistance has arisen to potent peptidomimetic drugs necessitating the further development of novel chemical backbones for diversity based chemistry focused on probing the active site for inhibitor interactions and binding modes that evade protease resistance. AQ148 is a potent inhibitor of HIV-1 PR and represents a new class of transition state analogues incorporating an aminimide peptide isostere. A 3-D crystallographic structure of AQ148, a tetrapeptide isostere, has been determined in complex with its target HIV-1 PR to a resolution of 2.5 Å and used to evaluate the specific structural determinants of AQ148 potency and to correlate structure–activity relationships within the class of related compounds. AQ148 is a competitive inhibitor of HIV-1 PR with a K_i value of 137 nM. Twenty-nine derivatives have been synthesized and chemical modifications have been made at the P1, P2, P1', and P2' sites. The atomic resolution structure of AQ148 bound to HIV-1 PR reveals both an inhibitor binding mode that closely resembles that of other peptidomimetic inhibitors and specific protein/inhibitor interactions that correlate with structure–activity relationships. The structure provides the basis for the design, synthesis and evaluation of the next generation of hydroxyethyl aminimide inhibitors. The aminimide peptide isostere is a scaffold with favorable biological properties well suited to both the combinatorial methods of peptidomimesis and the rational design of potent and specific substrate-based analogues. Copyright © 1996 Elsevier Science Ltd

Introduction

The human immunodeficiency virus (HIV) has been implicated as the causative agent of acquired immune deficiency syndrome (AIDS).¹ The RNA genome of the HIV retrovirus encodes an aspartic protease known as HIV-1 PR.² This protease is required for maturation and proliferation of the infectious virion. The essential role of HIV-1 PR is to cleave the virally encoded gag and gag-pol polyproteins into functional enzymes and structural proteins.³ HIV-1 PR is considered to be a promising target for the design of anti-AIDS drugs since inhibition leads to loss of viable viral particles in infected cells. The X-ray crystal structure of the HIV-1 PR has been solved and shows that the enzyme is formed by the homodimerization of a 99 amino acid polypeptide to form a C2 symmetric active site at the interface of the two subunits. Each subunit contributes one of two symmetrically disposed aspartic acid residues required for catalysis.⁴ The structure clearly illustrates the extended active site of the protein, which incorporates processing subsites of S4-S3'.⁵ Independent substrate cleavage assays have indicated that substrate specificity of HIV-1 PR is significantly determined by subsites S2–S2'.⁶

Numerous inhibitors of HIV-1 PR have been reported in the literature.⁷ Structure-based inhibitor design has focused on either transition state analogues,⁸ substrate analogues; or de novo designed compounds.⁹ The design of transition state analogue inhibitors of HIV-1 PR has centered on attempts to replace the scissile amide bond with nonhydrolysable peptide isosteres such as reduced amides, hydroxyethylamines, and statine derivatives. Here we report the design, synthesis, and crystallographically determined binding mode of a new transition state analogue inhibitor containing a hydroxyethyl aminimide moiety (Fig. 1) as a peptide isostere. The inhibitor is a novel lead compound that was designed from first principles based on our knowledge of the HIV-1 PR active site structure and binding preferences, synthesized and characterized on a time scale of less than 1 year. This compound is a starting point for the development of a more potent inhibitor that may demonstrate efficacy as an anti-AIDS drug.

Hydroxyethyl aminimides are generally prepared from the one-step reaction of an ester or acid chloride, a hydrazine, and an epoxide (W. J. Middleton, United States Patent 3,963,776 and B. M. Culbertson, United States Patent 3,963,703), or alternatively from the alkylation of a disubstituted hydrazide through the opening of an epoxide (R. A. Grimm, United States

Key words: aspartyl protease, aminimide, protease inhibitor, human immunodeficiency virus, lead compound.

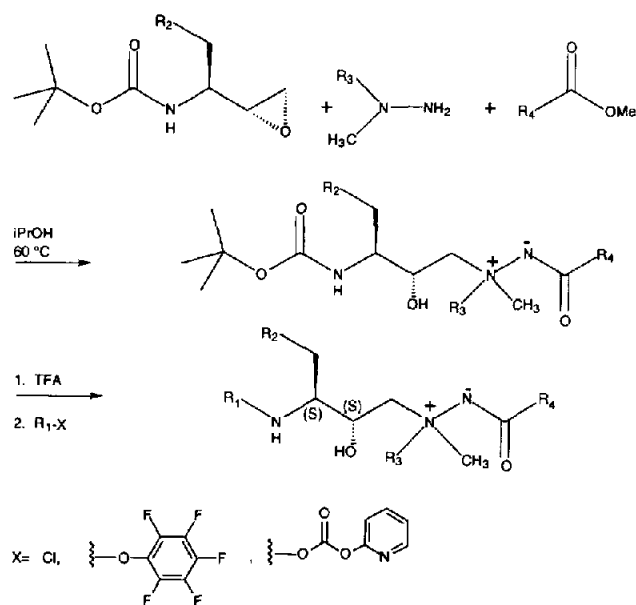


Figure 1. The reaction scheme for the synthesis of a zwitterionic hydroxyethyl aminimide backbone with four positions where functional groups R_1 – R_4 have been introduced.

Patent 3,850,969; Fig. 1). Aminimides possess a diversity of interesting properties and have been studied for a variety of industrial and biological applications. Hydroxyaminimides have proven efficacious as vasodilators¹⁰ and the aminimide besulphamide has significant diuretic and antihypertensive activity.¹¹ Recently, the crystallographic structure of elastase bound to an aminimide inhibitor has been determined.¹²

Results

Inhibition characteristics

AQ148 inhibits HIV-1 PR, HIV-2 PR, and SIV PR equally, but demonstrates no inhibitory effects on the human aspartyl proteases renin and pepsin (Table 1). Table 2 shows aminimide isosteres synthesized and IC_{50} values obtained. A direct comparison is made with the IC_{50} value measured for the known potent peptidomimetic inhibitor, acetyl pepstatin (IC_{50} =200 nM). The solubility of some of these compounds was increased by replacing the *t*-BOC group at P2 with heterocyclic moieties. The binding affinity and cellular toxicity was not significantly affected by this substitution (AQ173 and AQ169). The effects of AQ148 and AQ169 on HIV-1 viral polypeptide processing, as analysed in a cell culture system that constitutively produces nonenveloped HIV-1 particles,¹³ are currently under investigation. Preliminary results show that the inhibitor AQ148 exhibits no toxicity to cells in the range of 50–250 μ M over a time period of 24–48 h.

Inhibitor binding mode

AQ148 is a peptide isostere backbone bearing hydrogen bond donor and acceptor atoms arranged to interact with key donors and acceptors in the active site

Table 1. Inhibitory effects of AQ148 on various aspartyl proteases

Protease	NaCl Conditions in assay	Activity detection	IC_{50} (μ M) ^a
HIV-1	1 M	HPLC	0.2
HIV-1	1 M	Fluoroskan	1.5
HIV-2	1 M	Fluoroskan	3.4
SIV	1 M	Fluoroskan	5
Pepsin	-	HPLC	N.I. at 250
Renin	-	HPLC	N.I. at 250
HIV-1	0.2 M	Fluoroskan	1.75

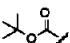
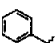
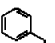
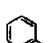


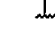

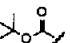
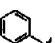
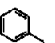




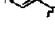
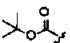
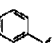
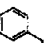
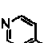


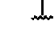
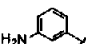
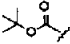
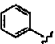
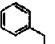


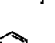

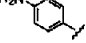
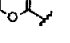
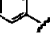
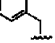

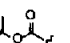
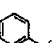
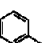
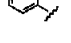


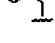

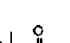


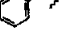
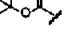
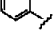
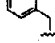
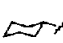
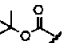
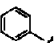
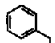

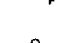



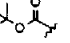
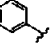
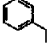

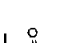


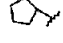
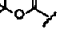
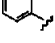
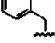
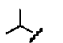
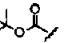
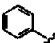
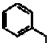
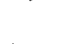


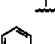
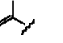
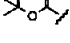
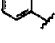
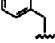

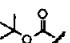
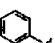
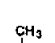
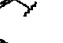
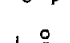


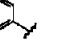
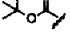
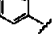
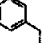

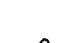


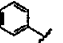
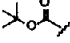
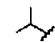
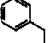




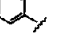
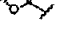
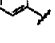
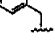

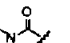
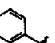
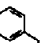
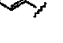
^aN.I., no inhibition.

and four hydrophobic substituents arranged to occupy generally hydrophobic subsites (S2, S1, S1', and S2') on the enzyme. The difference electron density for AQ148 shows clear and detailed features which allowed unambiguous placement and successful refinement of the inhibitor model. Refinement of the inhibitor model in the twofold related orientation generated using the C2 symmetry of the protein resulted in a poorer fit between the model and the electron density and an unreasonable van der Waals interaction between the oxygens of the catalytic aspartic acid residues and the amide methyl group of AQ148. The initial unbiased electron density map, calculated using phases from the rigid body refined protein model prior to the inclusion of AQ148 is shown in Figure 2 with the final, refined AQ148 model and the catalytic aspartic acid residues for reference. Most notable is that although nearly every nonhydrogen atom of the inhibitor lies within the 2.5 sigma electron density envelope, the phenyl ring at the P2' position has diminished electron density indicating that this substituent is less ordered than the rest of the molecule.

The protein C α atoms were used to guide the least-squares superposition of the AQ148 bound HIV-1 PR structure and the 7HVP structure¹⁴ from the Protein Data Bank¹⁵ to compare the binding mode of AQ148 to that of the peptidomimetic inhibitor JG365. The C α atoms of the two structures superimpose with an RMS deviation of 0.77 Å. AQ148 and the peptidomimetic inhibitor JG365 from the 7HVP structure are shown after superposition in Figure 3. A striking observation from the overlapped structures is that the oxygen atoms of AQ148 superimpose very closely with analogous oxygen atoms of JG365. The hydroxyl oxygen of AQ148 (Fig. 3) is 0.76 Å from the analogous atom in JG365 while the carbonyl oxygens adjacent to the *t*-BOC group at P2 and the phenyl ring at P2' are 0.76 and 1.53 Å from the analogous carbonyl oxygens in JG365.

The AQ148 peptide isostere backbone presents oxygen and nitrogen atoms which mimic the hydrogen bonding roles of the amide nitrogens and carbonyl oxygens in the natural substrate, but provide resistance to proteolysis. The AQ148 carbonyl oxygen, adjacent to the

Table 2. Chemical structures and inhibitory activities of compounds in the AQ148 family

Inhibitor	Stereochemistry at the quaternary N	R ₁	R ₂	R ₃	R ₄	IC ₅₀ (μM)
AQ148	<i>R</i>					0.2 ± 0.02
AQ149	<i>S</i>					1.2 ± 0.2
AQ150	<i>R</i>					9.5 ± 1.0
AQ151	<i>S</i>					34 ± 3.0
AQ152	<i>R</i>					4.5 ± 0.5
AQ153	<i>S</i>					26 ± 2.0
AQ154	Mix					2.4 ± 0.3
AQ155	Mix					45 ± 5.0
AQ156	<i>R</i>					5.0 ± 0.5
AQ157	<i>S</i>					12.5 ± 1.0
AQ158	<i>R</i>					1.0 ± 0.5
AQ159	<i>R</i>					1.0 ± 0.2
AQ160	<i>S</i>					60 ± 5.0
AQ161	<i>R</i>					3.0 ± 0.3
AQ162	<i>R</i>					0.85 ± 0.05
AQ163	<i>R</i>					2.5 ± 0.3
AQ164	<i>R</i>					5.0 ± 0.7
AQ165	<i>R</i>					14 ± 0.2
AQ166	<i>R</i>					0.25 ± 0.3
AQ167	<i>S</i>					2.3 ± 0.3
AQ168	<i>R</i>					5.0 ± 0.5
AQ169	<i>R</i>					0.21 ± 0.03
AQ170	<i>R</i>					6.0 ± 0.6
AQ171	<i>R</i>					3.0 ± 0.5
AQ172	<i>R</i>					185 ± 15
AQ173	<i>R</i>					0.5 ± 0.1
AQ174	<i>R</i>					34 ± 4.0
AQ175	<i>R</i>					0.75 ± 0.08
AQ176	<i>S</i>					39 ± 4.0

Functional groups R₁–R₄ are as in Figure 1.

phenyl ring at P2', together with the amide nitrogens of Ile 50 and Ile 150 coordinate a well ordered water molecule (Fig. 4). A similar water molecule is coordinated by the same amide nitrogens and the carbonyl oxygens of the P2 and P1' residues in the peptidomimetic bound structures of HIV-1 PR. In the AQ148 bound structure, the carbonyl oxygen at P2' is 2.96 Å from the amide nitrogen of Ile 150, close enough for a strong hydrogen bond. The distance between analogous atoms in other HIV-1/inhibitor complexes is greater than 4 Å. The AQ148 amide nitrogen between the *t*-BOC group at P2 and the phenyl ring at P1 is hydrogen bonded to the carbonyl oxygen of Gly 27. An analogous hydrogen bond is formed between the P1 amide nitrogen and the carbonyl oxygen of Gly 27 in peptidomimetic bound structures. The nitrogen atoms of the aminimide group do not interact with any protein atoms, although an ordered water molecule is coordinated between the imide nitrogen of the aminimide group and the backbone amide nitrogen of Asp 129 (Fig. 4). The Asp 129 amide nitrogen is hydrogen bonded to the carbonyl oxygen of the P2' residue in other peptidomimetic structures. The methyl group attached to the quaternary aminimide nitrogen is oriented toward the backbone carbonyl carbon of Gly 127. The carbonyl oxygen of Gly 127 is shifted away

from the inhibitor 1.1 Å relative to its position in the 7HVP structure to sterically accommodate the methyl group.

The hydrophobic substituents of AQ148 also superimpose with the side chains of the peptidomimetic inhibitor JG365 (Fig. 3). The phenyl group at the P1 position lies in the S1 subsite and extends toward the S3 subsite. The natural cleavage sites of HIV-1 PR almost invariably contain a hydrophobic residue at P1. In comparison to the bound conformation of the JG365 phenyl ring in the S1 subsite, the atoms of the AQ148 phenyl ring at P1 are shifted toward the S3 subsite by 1–1.4 Å. This phenyl ring lies in a pocket comprised of sidechain atoms from residues: Ile 50, Arg 108, Pro 181, and Val 182, and the backbone atoms of residues Gly 49 and Ile 50 [Fig. 5(a)].

The *t*-butyl containing *t*-BOC group at P2 occupies the S2 subsite. Other potent inhibitors of HIV-1 PR whose structures have been determined and published contain a *t*-BOC group at P2,^{16,17} a position occupied most commonly by a hydrophobic residue in natural substrates. The *t*-butyl group lies in a hydrophobic pocket comprised of the following residues: side chains of Val 32, Ile 47, Ile 84, and Ile 150 and backbone

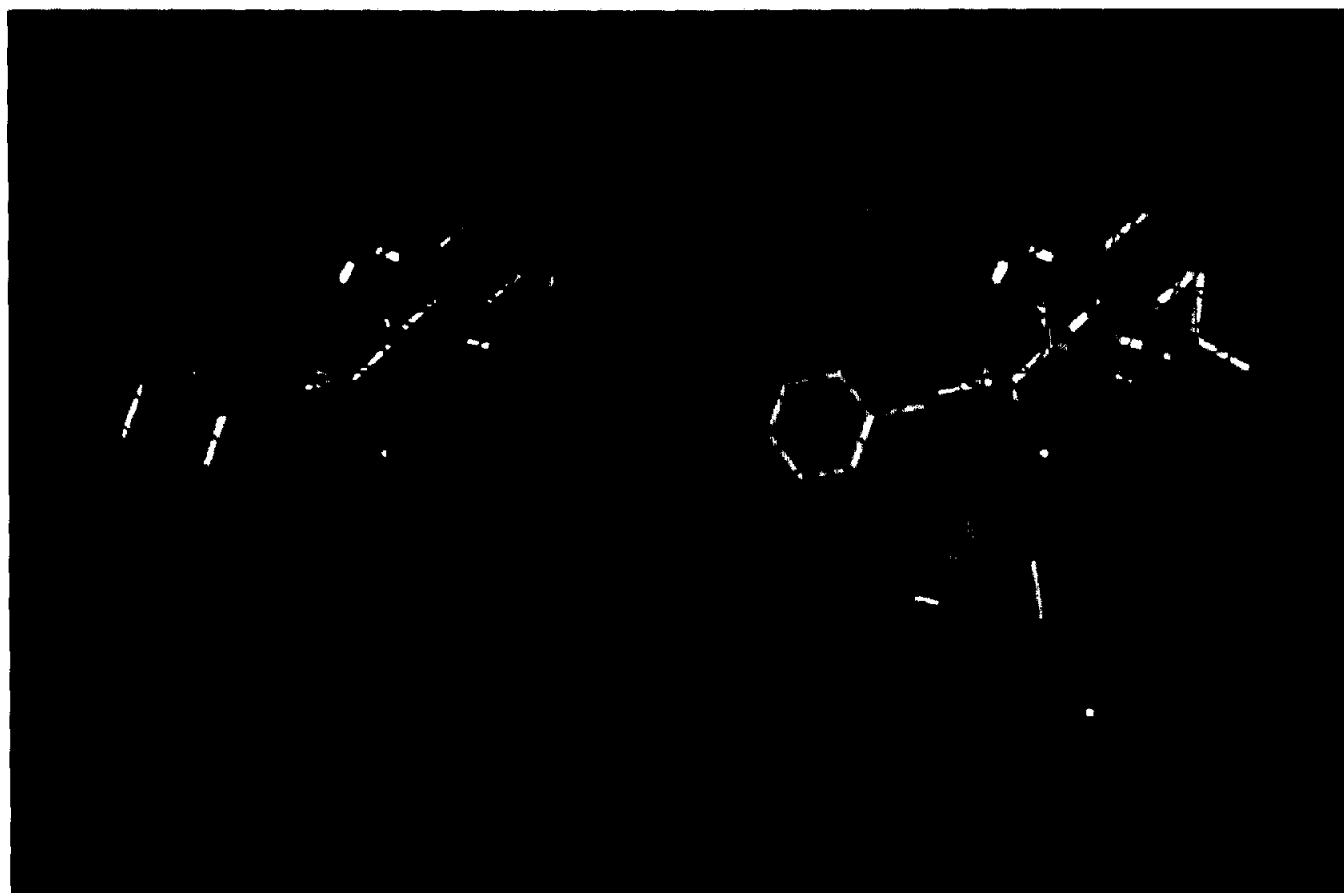


Figure 2. The bound conformation of AQ148 and the water molecule coordinated between the flap amide nitrogens (not shown) and the inhibitor. The atoms are colored by type: oxygen is red, nitrogen is blue, carbon is green and hydrogen is white. The unbiased, omit electron density map for the inhibitor and the bound water molecule is shown at a 2.5 sigma contour. The catalytic aspartic acid residues are shown for reference.

atoms of residues Asp 29, Asp 30, Thr 31, Gly 48, and Gly 49 [Fig. 5(b)].

The P1' phenyl ring lies in the S1' subsite and extends toward the S3' subsite. Again, natural cleavage sites of HIV-1 PR often contain a hydrophobic residue at P1'. The P1' phenyl ring lies in a pocket comprised of side-chain atoms from residues: Arg 8, Leu 23, Pro 81, Val 82, and Asp 129 and backbone atoms of Gly 149 [Fig. 5(c)].

In contrast to the P1, P1' and P2 substituents, which bind in or near their cognate subsite, the phenyl group at P2' binds above the S2' subsite, 2.1 Å from the analogous substituent at P2' in JG365. The phenyl ring occupies a hydrophobic pocket 'tucked' between the

flaps and created by displacement of the side chains of residues Ile 50 and Gly 51 by 2.2 and 1.2 Å, respectively, relative to their position in the 7HVP structure. The phenyl ring lies between the flaps in a pocket comprised of side chain atoms from residues: Ile 50, Ile 147, Ile 154, and backbone atoms of Gly 149 [Fig. 5(d)].

The individual *B* factors for the atoms in the structure are refined. The average *B* factor for nonhydrogen protein atoms is 18.5 Å² and the average *B* factor for nonhydrogen inhibitor atoms is 14.8 Å². However, the *B* factors for the atoms of the P2' phenyl ring are the highest of all the atoms in the inhibitor, 10–15 Å² higher than the average. This indicates that this substituent is disordered relative to the rest of the

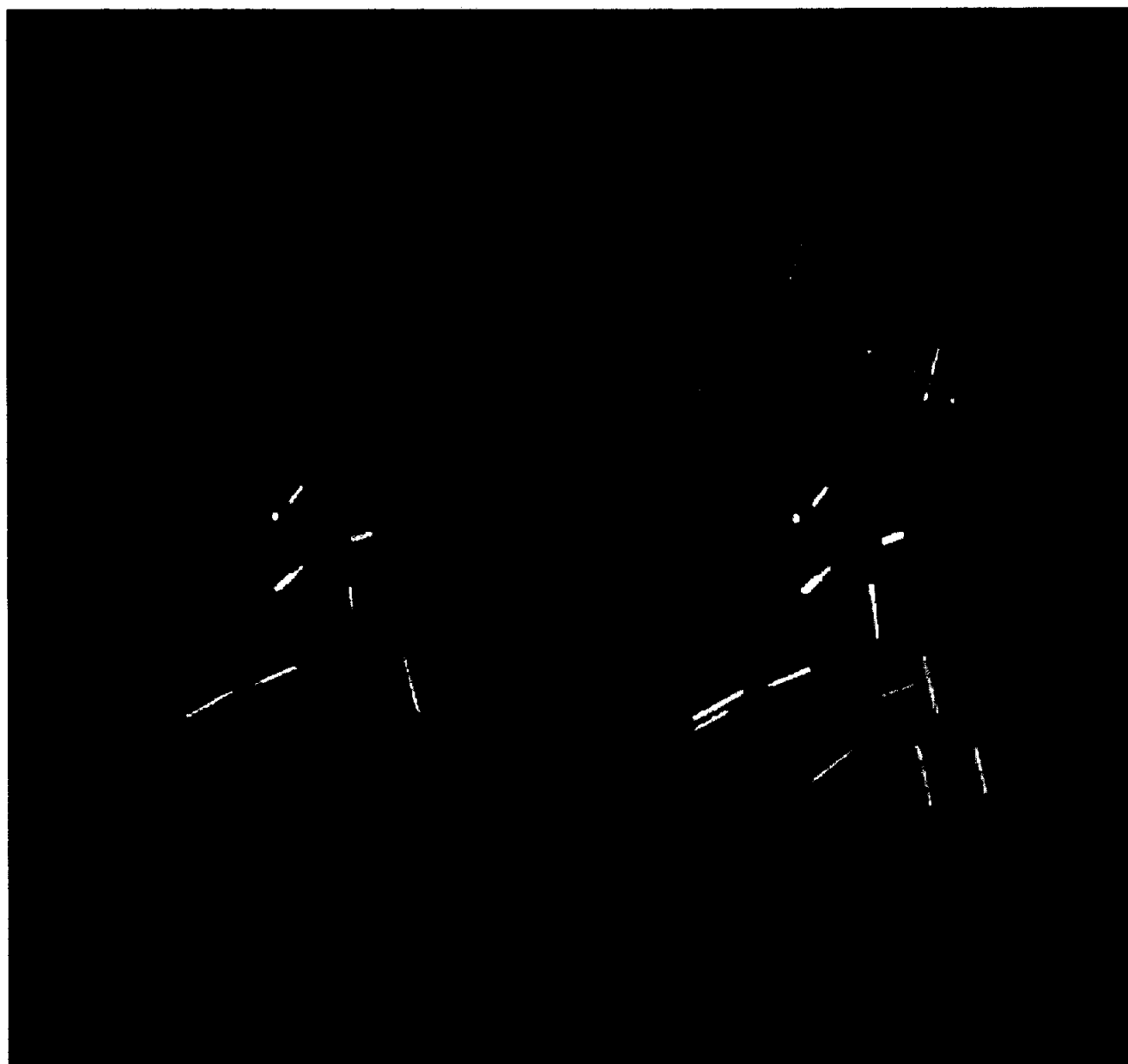


Figure 3. The bound conformation of the AQ148 molecule (colored by atom type as in Figure 1) is shown with the bound conformation of the peptidomimetic inhibitor JG365 (colored blue) after superposition of the respective protein Cas.

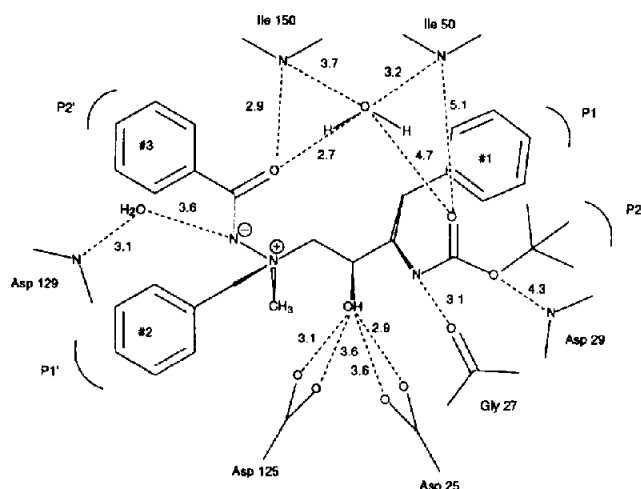


Figure 4. Schematic diagram of the bound conformation of AQ148. The dashed lines indicate distances in Å between nonhydrogen atoms.

inhibitor, corroborating the observation of weak electron density for this phenyl ring.

Theoretical model of inhibitor binding

Overall, the theoretical model developed for the binding of AQ 148 in the HIV-1 PR active site and used as the initial platform for inhibitor design shows excellent agreement with the crystallographically determined inhibitor/HIV-1 PR structure. The protein C α

atoms of the theoretical model show a 0.73 Å rms deviation from the crystallographic structure, whereas the main-chain atoms of the inhibitor differ by only 0.34 Å rms. The chirality of the quaternary nitrogen giving the best fit to the electron density is the *R* isomer, as correctly predicted by the model. The largest differences are restricted to the P2' residue, which binds unexpectedly close to the flap residues of the protein. The theoretical model did not predict the rearrangement of the flap residues and the formation of the hydrogen bond between the P2' carbonyl oxygen and the amide nitrogen of Ile 150. The distance between this nitrogen and the equivalent P1' carbonyl oxygen in other HIV-1 protease/inhibitor crystal structures in the PDB is typically 4–4.5 Å. The aminimide oxygen is also displaced ~ 1.6 Å from the position of the P1' carbonyl oxygen in these structures. Another significant difference between the model and the X-ray structure is the positioning of the P2' aromatic ring, which has its centroid in the X-ray structure displaced 2.6 Å relative to the model. This moves the ring away from the center of the S2' pocket, which is located almost 3.5 to 4 Å distant, based on all other available X-ray structures.

Structure–activity relationships

The strongest correlation between a specific structural feature of the inhibitor family described here (Table 2) and the potency of inhibition is for the stereochemistry at the quaternary nitrogen center. When the enantiomerically pure inhibitor is obtained, the compound with *R* stereochemistry has an IC₅₀ between 2.5- and 52-fold lower than for the corresponding *S* enantiomer. Structurally, the difference between *R* and *S* enantiomers might be viewed as a switch of the amide group at P2' for the phenyl group at P1', since the methyl group is sterically constrained in its binding pocket and the rest of the molecule presumably binds in the same fashion for both enantiomers. The P1' pocket shows a strong tendency to bind aromatic or hydrophobic groups and the phenyl ring is likely to provide better binding interactions than any of the amide groups.

Most of the analogues synthesized probe the binding specificity of the P2 and P2' functional groups presuming a binding mode similar to the expected orientation observed in the AQ148/HIV-1 PR structure. The *t*-BOC group at the P2 position in AQ148 occupies the S2 subsite in the bound enzyme structure. The S2 subsite usually accommodates branched residues and polar residues such as asparagine. The best alternative (AQ169 IC₅₀=0.21 μ M) at the P2 position is a tetrahydrofuran group which provides increased polarity relative to the *t*-BOC group. However, extension by a single methylene (AQ172 IC₅₀=185 μ M) abrogates the benefit afforded by this substituent probably due to unfavorable steric interactions with the side-chains of Ile 47 and Val 32. Most of the compounds with substitutions at P2' demonstrate low micromolar inhibition against HIV-1 PR. Since the AQ148 benzyl group at P2' binds somewhat removed from the formal S2' subsite and mediates

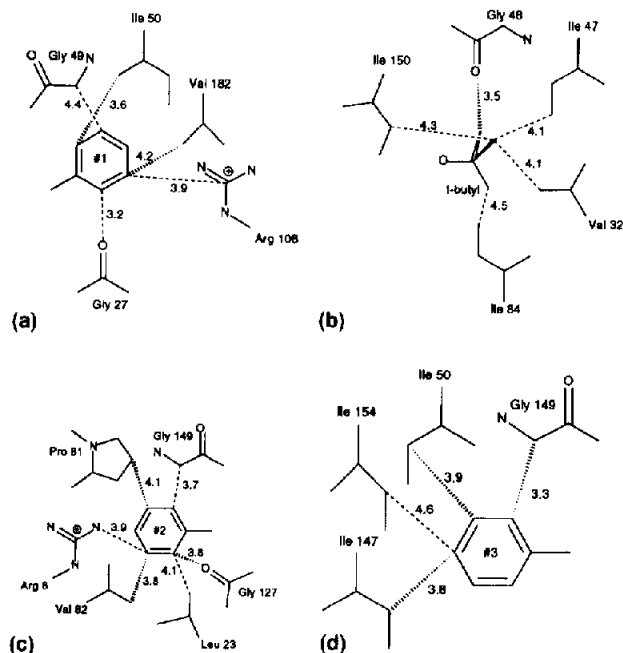


Figure 5. Schematic diagrams illustrate the binding mode and specify hydrogen bond distances and distances of closest approach between the inhibitor and the protein in Å. The phenyl substituents are numbered one, two, and three for reference as in Figure 4. (a) The phenyl ring at the P1 position. (b) The *t*-BOC substituent at the P2 position. (c) The phenyl ring at the P1' position. (d) The phenyl ring at the P2' position.

rearrangement of the flap residues, alterations were designed to be less bulky (AQ164, AQ163 and AQ161) and to direct the phenyl ring into the S2' subsite (AQ158). Also, specific hydrogen bonds from the P2' residue to the carbonyl oxygens of Gly 127 and Gly 148 have lead to potent inhibitors.^{18,19} Currently, new aminimide compounds are being designed to include an alkyl group in the P2' position with a hydrogen-bond donor to interact with the carbonyl oxygen of Gly 148.

Substituents at P1 and P1' are less varied. Phenyl rings at P1 and P1' are bound within the S1 and S1' subsites but extend toward the guanadinium head groups of Arg 108 and Arg 8, respectively, which flank the S3 and S3' subsites. Each of these arginines is involved in a salt bridge with a side-chain carboxylate of Asp 129 and Asp 29, respectively, and can make favorable interactions with inhibitors bearing polar atoms in the S3 and S3' subsites. A hydrogen bond acceptor on the meta position of either of these rings might interact with the nearby arginine residue.

Discussion

We describe the crystallographic structure of a novel peptide isostere bound by the enzyme active site it was designed to inhibit. The inhibitor is an aminimide scaffold that mimics the peptide backbone and enables the rapid and diverse juxtaposition of various substituents in a modular fashion. Peptidomimesis is a burgeoning field in search of novel backbone structures upon which to build peptide-like substituents that result in compounds with both specific binding and favorable biological properties characteristic of a useful drug. The aminimide scaffold has shown efficacy in other applications^{10,11} and presents the opportunity to improve biological properties such as solubility and bioavailability of a lead compound through the combinatorial chemistry route. The marriage of structure-based methods and diversity generating syntheses centered around the aminimide peptide isostere provides the means for expeditious discovery and inexpensive production of potent bioactive compounds which have efficacy and specificity toward a target peptidyl binding site.

A serious limitation to the effectiveness of HIV-1 PR inhibitors is the loss of antiviral sensitivity that results upon prolonged exposure of infected cells to the inhibitor. Several of the specific mutations which arise in HIV-1 PR and lead to inhibitor resistance have been identified²⁰ and a subset of these residues, Ile 47, Ile 54, Val 82, and Ile 84, lie directly adjacent to the bound AQ148 molecule. One mechanism of resistance appears to involve removal of a favorable hydrophobic interaction between the inhibitor and the protein active site through a mutation such as Val→Ala or Ile→Val. Since these four residues make several close contacts with the AQ148 molecule a similar pattern of resistance could arise in HIV-1 PR. However, the aminimide backbone described here bears four substituents,

each of which may be chemically altered in a structure-directed fashion for a resulting diversity of over 10⁶ compounds. Together, the crystallographic structure of the bound aminimide isostere, our current understanding of resistance mechanisms and the profound diversity of compounds attainable with this backbone provide the basis for generating aminimide HIV-1 PR inhibitors that are effective against the manifold forms of the protease.

Experimental

Inhibitor design and theoretical model of AQ148 binding

The inhibitors presented here were designed using an inhibitor model based on data from previous inhibition studies with HIV-1 PR and the published success of compounds possessing the hydroxyethylene dipeptide isostere.⁶ Compounds AQ148 and AQ149 were the first to be made, since it is well established that phenyl substituents at P1 and P1' are preferred. Compounds AQ165 and AQ168 were made to compare the structure-activity relationships (SAR) at P1 and P1' with the hydroxyethylene counterparts. A similar decrease in activity was noted for these analogues, supporting the premise that these hydroxyaminimides would bind in a fashion similar to the hydroxyethylene compounds. It was also noted that the activity of the R stereoisomer at the quaternary nitrogen was significantly greater than its epimer. Analogues AQ150–AQ157 varied the substituent at the P2' position to explore the possibility of acquiring better interaction through potential hydrogen bonding, since it is known that P2' can accommodate polar residues.²¹

A model of the most potent compound (AQ148) was constructed in the active site of HIV-1 protease using the available crystallographic data of complexes with other inhibitors. The highest resolution crystallographically determined structure of HIV-1 PR, 8HVP²² from the Brookhaven Protein Data Bank was used as basis for the model. An atomic model of AQ148 was positioned in the active-site of HIV-1 PR with a benzyl group at P1 and P1', a *t*-BOC group at P2 and a benzoyl group at P2'. The CVFF force field²³ was used in the DISCOVER program (Biosym Technologies) for all calculations pertaining to the theoretical model. Default atomic centered point charges were used for the inhibitor, but the barrier height for rotation about the N–N aminimide bond was adjusted to 8.5 kcal/mol in accordance with preliminary ab initio calculations (data not shown) performed using SPARTAN (Wavefunction, Inc). For reasons of computational efficiency, energy refinements of the protein/inhibitor model included all atoms of the inhibitor and those protein residues and crystallographic waters having any atom within 7 Å of any inhibitor atom. One of the catalytic aspartic acid residues (Asp 25) was modeled in the protonated state. A distance-dependent dielectric constant of 1R was used in the calculations and energy minimizations of the complexes were

considered converged when all components of the gradient were less than 10^{-3} kcal/mol/Å.

The energy-minimized inhibitor models in the presence of protein and in vacuo suggested that only the *R*-aminimide isomer of AQ148 is able to form stable interactions with protein residues and that no large conformational changes in the inhibitor were required in order to adopt the bound conformation. The P2' substituents were predicted to be within the S2' hydrophobic pocket. None of the aromatic substituents in the AQ150–AQ157 series had any potential hydrogen bonding interactions in the model which, with the possible exception of the *R* isomer of AQ154, fit the SAR data. To more thoroughly test the hydrophobic character at P2' a series of analogues AQ158–AQ164 were synthesized. These did not lead to any increase in activity, but did demonstrate that aromatic substituents α to the carbonyl were not required to obtain reasonable inhibition. The model further suggested that placing hydrogen bond donating groups at either *ortho* or *meta* positions on the aromatic system at P1' or at the P2' position β to the carbonyl using a *R*-chiral center α to this carbonyl could interact with O Gly 148. The activity of AQ166 seemed to support this premise, though activity was about the same as AQ148, perhaps due to the weaker hydrogen bonding capacity of aromatic amines as compared to their phenolic counterparts. Substitutions at the P2 position were the next most synthetically accessible and were made based primarily on the previously reported results of increased affinity using asparagine and (3*S*)-tetrahydrofuran urethanes at this position.²⁴

Chemical synthesis

Syntheses of compounds AQ148–AQ176 required the three building blocks for the aminimide: (1) methyl ester for the P2' position; (2) hydrazine for the P1' position; and (3) *t*-BOC protected epoxide for the P1 position. Modeling studies suggested that the preferred stereochemistry of our hydroxyethyl aminimide would be the (*S,S,R*) configuration. This necessitated the synthesis of the enantiomerically pure epoxides. Large quantities of the pure amino epoxides are prepared by the method of Luly et al.²⁵ When 1,1-disubstituted hydrazines, where the alkyl substituents are not identical, are used in the aminimide synthesis, the resulting quaternary nitrogen becomes a prochiral center. Since the epoxide opening by the hydrazine occurs in a stereo-random fashion, this mandates that both the (*S,S,R*) and (*S,S,S*) are formed in an essentially 1:1 ratio. In most cases, the diastereomers can be separated for independent testing via normal phase chromatography.

Unless stated otherwise, all materials were obtained from commercial suppliers and used without further purification. All silica gel column chromatography was performed using the method of Still, Kahn, and Mitra.²⁶ NMR samples were obtained in CDCl₃ unless stated otherwise. ¹H NMR spectra were obtained at 300.075 MHz on a Varian Gemini spectrometer.

Spectra are reported in δ values with shifts that are relative to tetramethylsilane at 0 ppm. Spectral data are reported by chemical shift, peak multiplicity (s, d, t, q, m), coupling constant, and integration values. All reported coupling constants are proton–proton couplings. ¹³C NMR spectra were obtained at 75.5 MHz on a Varian Gemini spectrometer. Chemical shifts are in δ values shifts reported relative to CDCl₃ at 77.0 ppm. Mass spectrometry was performed by either APICI (AP) or electrospray (ES) in the analytical facilities at ArQule, or by FAB at the microanalytical facility at the Harvard University chemistry department. MS data is reported as *m/z*.

Representative synthetic route to hydroxyethyl aminimide (AQ148). To an isopropanol solution of 1.84 g (7.00 mmol) of phenylamine derived epoxide (prepared using the method of Luly et al.²⁵) and 1.05 g (7.69 mmol) of 1-benzyl-1-methylhydrazine (synthesized from the procedure of Ohme and Preuschof²⁷) was added to 957 μ L (7.69 mmol) of methyl benzoate. The reaction was allowed to stir at 60 °C overnight. HPLC analysis of the crude reaction indicated the presence of two diastereomers, which was expected due to the fixed chirality of the hydroxyethyl component and the resulting quaternary nitrogen of the aminimide. The solvent was removed under reduced pressure, and the crude oil was purified via silica gel column chromatography to yield 500 mg of the (*S,S,R*) diastereomer. A sample for enzymological testing was acquired by further purifying compound AQ148 by double recrystallization, to yield 150 mg of a white product. The product was shown to be a single diastereomer by ¹H and ¹³C NMR and mass spectroscopy. Reverse-phase HPLC (C-8, 10–100% linear MeOH gradient with 0.1% TFA) also confirmed the presence of a single isomer. The (*S,S,S*) diastereomer (AQ149) was isolated by additional chromatography of fractions enriched in this isomer.

Representative synthetic procedure for the inhibitor: (*S,S,R*)-1-(2-(*N*-*t*-butoxycarbonyl)amino-2-benzyl-1-hydroxypropyl)-*N*-methyl-*N*-benzylaminobenzoylimide (AQ148). ¹H NMR (300 MHz): δ 1.43 (s, 9), 2.87–2.99 (m, 3), 3.21–3.29 (m, 1), 3.55 (s, 3), 3.55–3.60 (m, 1), 4.23 (d, 13.2, 1), 4.41 (d, 10.2, 1), 5.30 (d, 9.6, 1), 6.06 (d, 13.5, 1), 6.76 (d, 7.2, 2), 7.20–7.42 (m, 12), 7.86–7.89 (m, 2); ¹³C NMR (75.5 MHz): δ 169.81, 155.84, 138.22, 137.99, 132.01, 130.09, 129.93, 129.71, 129.29, 129.23, 128.77, 128.04, 127.22, 126.89, 79.76, 68.12, 64.86, 63.30, 55.13, 51.80, 38.77, 28.38; FABMS: *m/z* 504 (MH⁺) 526 (M+Na).

Representative procedure to modify the P2 position (AQ169). A sample of 59 mg (0.117 mmol) of AQ148 was stirred in neat TFA for 15 min at room temperature to remove the *t*-BOC protecting group. The TFA was removed under vacuum. A solution of 49 mg (0.234 mmol) of 2-hydroxypyridinium carbonate of (*S*)-3-hydroxytetrahydrofuran²⁸ in 400 μ L of CH₂Cl₂ was added to the crude amine, followed by addition of 50 μ L (0.359 mmol) of Et₃N. The reaction was stirred

at 40 °C for 15 h. The solvent was removed by rotary evaporation. The crude product was purified by silica gel chromatography using 2% MeOH/CH₂Cl₂ as eluant. Removal of solvent from the product containing fractions afforded 48 mg (79% yield) of a white foam. The product was characterized by ¹H and ¹³C NMR and MS.

Representative synthetic procedure for modifying the P2 position: (S,S,S)-1-(2-(N-2-hydroxytetrahydrofuran-ylcarbonyl) amino-2-benzyl-1-hydroxypropyl) -N-methyl-N-benzylaminobenzoylimide (AQ169). ¹H NMR: δ 1.92–2.04 (m, 1), 2.08–2.19 (m, 1), 2.90 (d, 13.2, 1), 2.99 (d, 7.8, 2), 3.20–3.28 (m, 1), 3.54 (s, 3), 3.59–3.67 (m, 1), 3.770–3.92 (m, 4), 4.25 (d, 13.5, 1), 4.43 (d, 9.9, 1), 5.50–5.55 (m, 1), 6.06 (d, 13.2, 1), 6.79 (d, 7.8, 2), 7.22–7.45 (m, 11), 7.87 (d, 7.5, 2); ¹³C NMR: δ 169.81, 155.91, 137.86, 131.95, 130.10, 129.93, 129.63, 129.26, 129.13, 128.79, 128.00, 127.18, 126.98, 75.51, 73.33, 67.95, 66.93, 64.75, 63.46, 55.55, 51.82, 38.67, 32.70; MS (ES⁺): *m/z* 518 (MH⁺).

(S,S,R)-1-(2-(N-*t*-Butoxycarbonyl)amino-2-benzyl-1-hydroxypropyl)-N-methyl-N-benzylaminobenzoylimide (AQ149). ¹H NMR: δ 1.44 (s, 9), 2.88–3.01 (m, 3), 3.49–3.61 (m, 1), 3.55 (s, 3), 3.71–3.79 (m, 1), 4.11 (d, 9.9, 1), 4.96 (d, 9.3, 1), 5.04 (d, 12.6, 1), 5.31 (d, 12.3, 1), 7.16–7.42 (m, 15), 7.83–7.86 (m, 2); ¹³C NMR (75.5 MHz): δ 170.17, 155.70, 138.02, 137.70, 132.61, 130.00, 129.43, 128.82, 128.46, 127.96, 127.27, 126.50, 125.26, 79.51, 69.41, 68.41, 66.13, 54.89, 49.01, 38.45, 28.33; MS (AP⁺): *m/z* 504 (MH⁺).

(S,S,R)-1-(2-(N-*t*-Butoxycarbonyl)amino-2-benzyl-1-hydroxypropyl)-N-methyl-N-benzylaminonicotinoylimide (AQ150). ¹H NMR (300 MHz): δ 1.44 (s, 9), 2.87–2.92 (m, 3), 1.53 (d, 12.9, 1), 3.54 (s, 3), 3.54–3.63 (m, 1), 3.71–3.79 (m, 1), 4.11 (d, 9.9, 1), 4.92 (d, 9.6, 1), 5.00 (d, 12.6, 1), 5.30 (d, 12.6, 1), 7.19–7.41 (m, 12), 8.08–8.12 (m, 1), 8.62–8.64 (m, 1), 9.05 (s, 1); ¹³C NMR (75.5 MHz): δ 168.15, 155.87, 150.70, 149.04, 138.14, 134.82, 132.03, 130.22, 129.67, 129.57, 129.33, 128.95, 128.78, 126.90, 122.92, 111.46, 79.85, 68.33, 65.83, 64.92, 63.77, 55.20, 51.86, 38.71, 28.37; FABMS: *m/z* 505 (MH⁺).

(S,S,S)-1-(2-(N-*t*-Butoxycarbonyl)amino-2-benzyl-1-hydroxypropyl)-N-methyl-N-benzylaminobenzoylimide (AQ151). ¹H NMR (300 MHz): δ 1.43 (s, 9), 2.95–2.99 (m, 3), 3.23–3.31 (m, 1), 3.44–3.51 (m, 1), 3.54 (s, 3), 3.51–3.61 (m, 1), 4.28 (d, 13.8, 1), 4.39 (d, 9.9, 1), 5.97 (d, 13.2, 1), 6.79 (d, 7.8, 2), 7.22–7.40 (m, 10), 8.14 (d, 7.8, 1), 8.63–8.64 (m, 1), 9.08 (s, 1); ¹³C NMR (75.5 MHz): δ 168.13, 155.85, 150.68, 149.02, 138.13, 134.80, 132.02, 130.20, 129.65, 129.56, 129.31, 128.94, 128.76, 126.88, 122.91, 79.83, 68.30, 64.93, 63.80, 55.18, 51.84, 38.70, 28.35; FABMS: *m/z* 505 (MH⁺).

(S,S,R)-1-(2-(N-*t*-Butoxycarbonyl)amino-2-benzyl-1-hydroxypropyl)-N-methyl-N-benzylamino-*i*-nicotinoylimide (AQ152). ¹H NMR (300 MHz): δ 1.43 (s, 9), 2.95–3.03

(m, 3), 3.22–3.30 (m, 1), 3.53 (s, 3), 3.60–3.62 (m, 1), 4.27 (d, 13.5, 1), 4.39 (d, 10.2, 1), 5.23 (d, 9.3, 1), 5.93 (d, 13.5, 1), 6.80 (d, 7.5, 2), 7.26–7.41 (m, 9), 7.69–7.71 (m, 2), 8.66–8.68 (m, 2); ¹³C NMR (75.5 MHz): δ 167.93, 149.78, 145.79, 138.14, 132.10, 130.32, 129.65, 129.36, 128.81, 126.94, 121.68, 79.91, 68.71, 68.37, 65.37, 55.31, 51.89, 38.77, 28.40. FABMS: *m/z* 505 (MH⁺).

(S,S,S)-1-(2-(N-*t*-Butoxycarbonyl)amino-2-benzyl-1-hydroxypropyl)-N-methyl-N-benzylamino-*i*-nicotinoylimide (AQ153). ¹H NMR (300 MHz): δ 1.43 (s, 9), 2.88–3.01 (m, 4), 3.54 (s, 3), 3.49–3.63 (m, 1), 3.73–3.78 (m, 1), 4.12 (d, 9.9, 1), 4.91–5.01 (m, 2), 5.30 (d, 12.6, 1), 7.15–7.43 (m, 10), 7.65–7.70 (m, 2), 8.63 (d, 6.3, 2); ¹³C NMR (75.5 MHz): δ 168.15, 149.97, 145.56, 137.58, 132.59, 130.23, 129.64, 129.34, 129.24, 129.07, 128.98, 128.93, 128.78, 128.53, 127.38, 126.92, 126.59, 121.55, 79.69, 69.51, 68.56, 66.21, 54.93, 48.99, 38.42, 28.34; FABMS: *m/z* 505 (MH⁺).

(S,S,R/S)-1-(2-(N-*t*-Butoxycarbonyl)amino-2-benzyl-1-hydroxypropyl)-N-methyl-N-benzylamino-*m*-aminobenzoylimide (AQ154). A 1:1 mixture of inseparable diastereomers: ¹H NMR (300 MHz): δ 1.42 and 1.43 (s, total 18), 2.86–2.98 (m, total 6), 3.19–3.27 (m, total 2), 3.52 and 3.53 (s, total 6), 3.52–3.62 (m, 1), 3.94–4.00 (m, 1), 4.08–4.13 (m, 1), 4.22 (d, 12.6, 1), 4.33–4.41 (m, 2), 4.94–5.02 (m, total 3), 5.20–5.34 (m, total 3), 6.03 (d, 13.8, 1), 6.72–6.77 (m, total 4), 7.11–7.42 (m, total 25); ¹³C NMR (75.5 MHz): δ 170.32, 169.94, 155.82, 155.72, 146.23, 146.19, 139.18, 139.12, 138.25, 138.22, 137.74, 135.77, 132.65, 132.00, 130.03, 129.98, 129.70, 129.48, 129.29, 129.25, 129.18, 129.05, 128.99, 128.90, 128.83, 128.74, 128.48, 117.62, 117.51, 116.63, 114.17, 79.23, 79.53, 69.39, 68.37, 66.13, 64.84, 63.26, 62.70, 55.12, 54.91, 51.76, 49.06, 41.63, 38.73, 38.50, 28.35; FABMS: *m/z* 519 (MH⁺).

(S,S,R/S)-1-(2-(N-*t*-Butoxycarbonyl)amino-2-benzyl-1-hydroxypropyl)-N-methyl-N-benzylamino-*p*-aminobenzoylimide (AQ155). ¹H NMR (300 MHz): δ 1.43 (s, 9), 1.92 (t, 6.6, 2), 2.8–2.99 (m, 8), 3.22 (t, 9.9, 1), 3.52 (s, 3), 3.52–3.59 (m, 2), 3.75–3.82 (m, 3), 3.98 (q, 6.3 and 13.7, 2), 4.20 (d, 13.2, 1), 4.36–4.42 (m, 2), 4.92 (bs, 2), 5.31 (d, 7.9, 1), 6.07 (d, 13.2, 1), 6.66 (d, 8.7, 2), 6.74 (d, 7.7, 2), 7.18–7.42 (m, 9), 7.70 (d, 8.6, 2). FABMS: *m/z* 519 (MH⁺).

(S,S,R)-1-(2-(N-*t*-Butoxycarbonyl)amino-2-benzyl-1-hydroxypropyl)-N-methyl-N-benzylamino-*p*-methoxybenzoylimide (AQ156). ¹H NMR (300 MHz): δ 1.43 (s, 9), 2.85–2.99 (m, 3), 3.20–3.28 (m, 1), 3.53 (s, 3), 3.53–3.59 (m, 1), 3.84 (s, 3), 4.22 (d, 14.1, 1), 4.41 (d, 10.5, 1), 5.29–5.31 (m, 1), 6.75 (d, 6.6, 2), 6.90 (d, 8.1, 1), 7.20–7.40 (m, 9), 7.83 (d, 8.4, 2); ¹³C NMR (75.5 MHz): δ 169.49, 161.10, 155.81, 138.21, 131.98, 130.40, 130.03, 129.70, 129.26, 128.75, 126.87, 113.26, 79.73, 67.99, 64.85, 63.31, 55.30, 55.08, 51.85, 38.75, 28.36; FABMS: *m/z* 534 (MH⁺).

(*S,S,S*)-1-(2-(*N*-*t*-Butoxycarbonyl)amino-2-benzyl-1-hydroxypropyl)-*N*-methyl-*N*-benzylamino-*p*-methoxybenzoylimide (AQ157). ^1H NMR (300 MHz): δ 1.44 (s, 9), 2.86–2.99 (m, 4), 3.46–3.83 (m, 4), 3.54 (s, 3), 3.83 (s, 3), 4.10 (d, 10.2, 1), 4.95 (d, 9.9, 1), 5.06 (d, 12.6, 1), 5.29 (d, 12.3, 1), 6.86–6.91 (m, 2), 7.17–7.42 (m, 10), 7.80–7.84 (m, 2); ^{13}C NMR (75.5 MHz): δ 169.89, 161.09, 155.70, 132.64, 129.99, 129.46, 129.29, 129.21, 128.96, 128.80, 128.75, 128.48, 128.37, 128.33, 126.52, 113.23, 79.54, 69.41, 68.54, 66.15, 55.28, 54.88, 49.09, 38.47, 28.35; MS (AP^+): m/z 534 (MH^+).

(*S,S,R*)-1-(2-(*N*-*t*-Butoxycarbonyl)amino-2-benzyl-1-hydroxypropyl)-*N*-methyl-*N*-benzylaminophenylacetyl-imide (AQ158). ^1H NMR (300 MHz): δ 1.41 (s, 9), 2.79 (d, 13.2, 1), 2.87–2.97 (m, 3), 3.06 (t, 13.1, 1), 3.36 (s, 3), 3.40 (s, 2), 3.48–3.57 (m, 1), 4.11 (d, 13.2, 1), 4.24 (d, 9.9, 1), 5.20 (t, d, 9.5, 1), 5.78 (d, 13.2, 1), 6.69 (d, 7.3, 2), 7.16–7.44 (m, 14); ^{13}C NMR: δ 174.11, 155.76, 138.23, 138.02, 132.59, 131.90, 129.96, 129.66, 129.25, 129.16, 129.11, 128.70, 128.45, 128.27, 126.82, 126.11, 79.67, 67.89, 64.64, 63.03, 55.13, 51.63, 44.37, 38.73, 28.34; MS (ES^+): m/z 518 (MH^+).

(*S,S,R*)-1-(2-(*N*-*t*-Butoxycarbonyl)amino-2-benzyl-1-hydroxypropyl)-*N*-methyl-*N*-benzylaminocyclohexylcarbonylimide (AQ159). ^1H NMR (300 MHz): δ 1.21–1.31 (m, 4), 1.41 (s, 9), 1.46–1.86 (m, 6), 1.98–2.06 (m, 1), 2.76 (d, 12.0, 1), 2.93–2.98 (m, 2), 3.04–3.11 (m, 1), 3.38 (s, 3), 3.52–3.57 (m, 1), 4.09 (d, 12.9, 1), 3.33 (d, 10.2, 1), 5.26 (d, 9.6, 1), 5.89 (d, 13.5, 1), 6.71 (d, 7.2, 2), 6.70–7.43 (m, 9); ^{13}C NMR (75.5 MHz): δ 178.89, 155.77, 138.27, 131.91, 129.92, 129.67, 129.38, 129.18, 128.73, 126.82, 79.67, 67.44, 64.78, 62.76, 55.06, 51.61, 45.81, 38.82, 30.48, 30.33, 28.35, 26.24, 26.17; MS (AP^+): m/z 510 (MH^+).

(*S,S,S*)-1-(2-(*N*-*t*-Butoxycarbonyl)amino-2-benzyl-1-hydroxypropyl)-*N*-methyl-*N*-benzylaminocyclohexylcarbonylimide (AQ160). ^1H NMR: δ 1.18–1.41 (m, 4), 1.41 (s, 9), 1.64–1.86 (m, 6), 1.98–2.03 (m, 1), 2.82–2.91 (m, 3), 3.41 (s, 3), 3.41–3.72 (m, 1), 3.70–3.72 (m, 1), 4.06 (d, 9.9, 1), 4.91 (d, 12.3, 2), 5.15 (d, 12.3, 1), 7.19–7.40 (m, 11); ^{13}C NMR (75.5 MHz): δ 179.21, 155.66, 137.79, 132.64, 129.95, 129.25, 128.75, 128.45, 128.35, 126.48, 79.45, 68.82, 68.29, 66.24, 54.78, 48.75, 45.77, 38.57, 30.47, 30.26, 28.24, 26.29, 26.21; MS (AP^-): m/z 510 (MH^+).

(*S,S,R*)-1-(2-(*N*-*t*-Butoxycarbonyl)amino-2-benzyl-1-hydroxypropyl)-*N*-methyl-*N*-benzylaminocyclopropylcarbonylimide (AQ161). ^1H NMR: δ 0.58–0.62 (m, 2), 0.77–0.81 (m, 2), 1.42 (s, 9), 2.77 (d, 13.2, 1), 2.90–2.98 (m, 2), 3.09–3.17 (m, 1), 3.39 (s, 3), 3.51–3.58 (m, 1), 4.15 (d, 13.2, 1), 4.36 (d, 9.9, 1), 5.28 (d, 9.9, 1), 5.85 (d, 13.2, 1), 6.69 (d, 7.2, 2), 7.17–7.46 (m, 8); ^{13}C NMR: δ 175.61, 155.77, 138.28, 131.92, 129.97, 129.70, 129.48, 129.32, 129.22, 129.10, 128.93, 128.76, 128.61, 128.48, 128.39, 126.86, 79.66, 67.52, 64.75, 63.19, 55.05, 51.77, 38.82, 28.36, 14.90, 5.60; MS (AP^+): m/z 468.

(*S,S,R*)-1-(2-(*N*-*t*-Butoxycarbonyl)amino-2-benzyl-1-hydroxypropyl)-*N*-methyl-*N*-benzylaminocyclopentylcarbonylimide (AQ162). ^1H NMR (300 MHz): δ 1.41 (s, 9), 1.54–1.87 (m, 8), 2.48–2.54 (m, 1), 2.76 (d, 13.2, 1), 2.93–3.00 (m, 2), 3.08 (t, 12.6, 1), 3.39 (s, 3), 3.51–3.57 (m, 1), 4.11 (d, 13.9, 1), 4.33 (d, 9.9, 1), 5.25 (d, 9.3, 1), 5.89 (d, 13.6, 1), 7.72 (d, 7.6, 2), 7.17–7.42 (m, 9); ^{13}C NMR: δ 178.87, 155.78, 138.28, 131.92, 129.92, 129.68, 129.38, 129.19, 128.73, 126.82, 79.67, 67.44, 64.78, 62.80, 55.07, 51.60, 46.09, 38.82, 30.84, 30.71, 28.36, 26.08; MS (AP^+): m/z 496 (MH^+).

(*S,S,R*)-1-(2-(*N*-*t*-Butoxycarbonyl)amino-2-benzyl-1-hydroxypropyl)-*N*-methyl-*N*-benzylamino-*i*-propylcarbonylimide (AQ163). ^1H NMR: δ 1.12 (d, 2.1, 3), 1.14 (d, 2.1, 3), 1.42 (s, 9), 2.28–2.39 (m, 1), 2.77 (d, 13.5, 1), 2.94–2.97 (m, 2), 3.04–3.12 (m, 1), 3.39 (s, 3), 3.51–3.60 (m, 1), 4.10 (d, 13.2, 1), 4.33 (d, 10.2, 1), 5.25 (d, 9.6, 1), 5.88 (d, 13.2, 1), 6.72 (d, 7.2, 2), 7.18–7.45 (m, 8); ^{13}C NMR: δ 179.72, 155.78, 138.28, 131.92, 129.94, 129.67, 129.35, 129.19, 128.73, 126.82, 79.68, 67.50, 64.76, 62.76, 55.08, 52.55, 38.81, 35.57, 28.35, 20.35, 20.21; MS (AP^+): m/z 470 (MH^+).

(*S,S,R*)-1-(2-(*N*-*t*-Butoxycarbonyl)amino-2-benzyl-1-hydroxypropyl)-*N*-methyl-*N*-benzylaminomethacrylimide (AQ164). ^1H NMR: δ 1.42 (s, 9), 1.95 (s, 3), 2.82 (d, 12.9, 1), 2.94–2.97 (m, 2), 3.10–3.18 (m, 1), 3.45 (s, 3), 3.52–3.60 (m, 1), 4.13 (d, 13.5, 1), 4.34 (d, 10.5, 1), 5.19 (s, 1), 5.24 (d, 9.9, 1), 5.84 (s, 1), 5.95 (d, 13.2, 1), 6.72 (d, 6.9, 2), 7.19–7.45 (m, 8); ^{13}C NMR: δ 170.74, 155.79, 142.46, 138.24, 131.95, 130.03, 129.69, 129.46, 129.25, 129.19, 128.75, 126.86, 118.23, 79.72, 68.00, 64.70, 62.80, 55.10, 51.53, 38.76, 28.36, 19.44; MS (AP^-): m/z 468 (MH^+).

(*S,S*)-1-(2-(*N*-*t*-Butoxycarbonyl)amino-2-benzyl-1-hydroxypropyl)-*N,N*-dimethylaminobenzoylimide (AQ165). ^1H NMR (300 MHz): δ 1.40 (s, 9), 2.93–2.97 (m, 2), 3.13 (d, 13.2, 1), 3.54 (s, 3), 3.62 (s, 3), 3.66 (m, 1), 3.75–3.90 (m, 1), 4.20 (d, 10.2, 1), 5.11 (d, 9.0, 1), 7.20–7.38 (m, 8), 7.83 (d, 7.8, 2); ^{13}C NMR (75.5 MHz): δ 169.99, 155.90, 137.69, 129.88, 129.36, 128.54, 127.93, 127.17, 126.56, 79.77, 73.96, 66.38, 55.19, 54.97, 50.63, 38.57, 28.30; FABMS: m/z 428 (MH^+), 450 ($\text{M} + \text{Na}$).

(*S,S,R*)-1-(2-(*N*-*t*-Butoxycarbonyl)amino-2-(2-amino-benzyl)-1-hydroxypropyl)-*N*-methyl-*N*-benzylaminobenzoylimide (AQ166). ^1H NMR (300 MHz): δ 1.44 (s, 9), 2.95–3.01 (m, 3), 3.22–3.29 (m, 1), 3.55 (s, 3), 3.55–3.57 (m, 1), 4.14 (d, 13.8, 1), 4.45 (d, 9.9, 1), 5.32 (d, 9.3, 1), 5.94–5.99 (m, 2), 6.18 (d, 7.5, 1), 6.62 (d, 8.1, 1), 6.97–7.02 (m, 1), 7.27–7.45 (m, 9), 7.86–7.89 (m, 2); ^{13}C NMR (75.5 MHz): δ 169.66, 155.81, 147.09, 138.51, 138.03, 130.13, 130.055, 129.89, 129.80, 128.74, 128.02, 127.19, 126.82, 121.71, 117.78, 116.26, 79.74, 67.97, 64.77, 63.28, 55.18, 51.88, 38.76, 28.38; MS (AP^-): m/z 519 (MH^+).

(*S,S,S*)-1-(2-(*N*-*t*-Butoxycarbonyl)-amino-2-(2-amino-benzyl)-1-hydroxy-propyl)-*N*-methyl-*N*-benzylamino-

benzoylimide (AQ167). ^1H NMR (300MHz): δ 1.44 (s, 9), 2.89–2.93 (m, 3), 3.06 (d, 12.6, 1), 3.50 (s, 3), 3.50–3.58 (m, 1), 3.70–3.75 (m, 1), 4.09 (d, 9.9, 1), 4.94 (d, 12.6, 1), 5.00 (d, 9.6, 1), 5.21 (d, 11.7, 1), 6.70–6.74 (m, 2), 7.10–7.42 (m, 14), 7.85–7.88 (m, 2); ^{13}C NMR (75.5 MHz): δ 170.10, 155.76, 146.93, 137.73, 130.12, 129.84, 129.78, 129.67, 129.41, 129.30, 129.20, 128.74, 128.49, 128.00, 127.22, 126.51, 122.45, 118.93, 116.50, 79.52, 69.69, 68.95, 66.20, 54.93, 48.53, 38.50, 28.38; MS (AP^+): m/z 519 (MH^+).

(S,S,R)-1-(2-(N-*t*-Butoxycarbonyl)-amino-2-*i*-propyl-1-hydroxypropyl)-N-methyl-N-benzylaminobenzoylimide (AQ168). ^1H NMR (300 MHz): δ 0.99 (d, 8.4, 6) 1.42 (s, 9), 1.55–1.59 (m, 1), 3.22–3.409 (m, 3), 3.56 (s, 3), 3.60–3.65 (m, 1), 4.36 (d, 9.3, 1), 4.74 (d, 13.2, 1), 4.90 (d, 9.0, 1), 5.94 (d, 12.9, 1), 7.67–4.46 (m, 9), 7.87 (d, 7.8, 2); ^{13}C NMR (75.5 MHz): δ 170.04, 155.99, 138.08, 132.34, 130.30, 129.84, 129.71, 129.34, 127.99, 127.23, 79.49, 68.70, 68.53, 63.98, 52.49, 51.25, 41.95, 28.35, 24.76, 22.84, 22.32; MS (AP^+): m/z 470 (MH^+).

(S,S,R)-1-(2-(N-Morpholinocarbonyl)amino-2-benzyl-1-hydroxypropyl)-N-methyl-N-benzylaminobenzoylimide (AQ170). ^1H NMR: δ 2.91–3.05 (m, 4), 3.17–3.25 (m, 1), 3.35 (q, 5.1, 4), 3.53 (s, 3), 3.68 (t, 5.1, 4), 3.85–3.91 (m, 1), 4.25 (d, 13.2, 1), 4.45 (d, 10.2, 1), 5.27 (d, 8.7, 1), 6.02 (d, 13.2, 1), 6.78 (d, 7.5, 2), 7.21–7.45 (m, 11), 7.87 (d, 7.8, 2); ^{13}C NMR: δ 169.71, 157.29, 138.28, 132.06, 130.17, 129.68, 129.28, 128.96, 128.77, 128.07, 127.25, 126.90, 68.29, 66.40, 65.06, 55.05, 53.52, 51.94, 44.03, 41.85, 38.98; MS (ES^+): m/z 517 (MH^+).

(S,S,R)-1-(2-(N-4-Hydroxytetrahydropyranylcabonyl)-amino-2-benzyl-1-hydroxypropyl)-N-methyl-N-benzylaminobenzoylimide (AQ171). ^1H NMR: δ 1.59–1.70 (m, 2), 1.88–1.92 (m, 2), 2.90 (d, 13.2, 1), 2.98–3.01 (m, 2), 3.21–3.29 (m, 1), 3.48–3.68 (m, 3), 3.55 (s, 3), 3.86–3.94 (m, 2), 4.25 (d, 13.2, 1), 4.44 (d, 9.9, 1), 4.74–4.81 (m, 1), 5.46 (d, 9.6, 1), 6.07 (d, 13.2, 1), 6.78 (d, 7.2, 2), 7.22–7.45 (m, 11), 7.86–7.89 (m, 2); ^{13}C NMR: δ 169.83, 155.79, 137.94, 131.98, 130.12, 129.96, 129.64, 129.28, 129.16, 128.80, 128.03, 127.18, 126.96, 69.92, 68.03, 65.32, 64.87, 63.49, 55.52, 51.85, 38.70, 32.05; MS (AP^+): m/z 532 (MH^+).

(S,S,R)-1-(2-(N-3-Methoxytetrahydrofuranylcabonyl)-amino-2-benzyl-1-hydroxypropyl)-N-methyl-N-benzylaminobenzoylimide (AQ172). ^1H NMR: δ 1.38–1.47 (m, 2), 1.58–1.65 (m, 1), 1.99–2.05 (m, 1), 2.50–2.58 (m, 1), 2.85–2.95 (m, 1), 2.99 (d, 7.8, 2), 3.21–3.29 (m, 1), 3.55 (s, 3), 3.59–3.92 (m, 4), 3.99–4.01 (m, 1), 4.06–4.13 (m, 1), 4.25 (d, 13.2, 1), 4.42 (d, 9.9, 1), 5.45 (d, 9.3, 1), 6.06 (d, 13.2, 6.78 (d, 7.2, 2), 7.22–7.45 (m, 11), 7.87 (d, 7.5, 2); ^{13}C NMR: δ 169.80, 156.31, 137.88, 131.99, 130.17, 130.04, 129.98, 129.65, 129.55, 129.31, 129.09, 129.05, 128.82, 128.05, 127.22, 127.00, 70.47, 68.05, 67.71, 67.68, 66.56, 64.75, 55.56, 51.90, 38.73, 38.55, 28.85; MS (ES^+) 532 m/z (MH^+).

(S,S,R)-1-(2-(N-Carbobenzoxy)amino-2-benzyl-1-hydroxypropyl)-N-methyl-N-benzylaminobenzoylimide

(AQ173). ^1H NMR (300 MHz): δ 2.88 (d, 13.2, 1), 3.00 (d, 8.7, 1), 3.20–3.24 (m, 1), 3.45–3.64 (m, 2), 3.50 (s, 3), 3.65–3.70 (m, 1), 4.22 (d, 13.2, 1), 4.41 (d, 10.5, 1), 5.08 (s, 2), 5.57 (d, 9.6, 1), 6.04 (d, 13.5, 1), 6.77 (d, 7.2, 2), 7.21–7.40 (m, 16), 7.84–7.87 (m, 2); ^{13}C NMR (75 MHz): δ 169.81, 156.26, 137.94, 136.30, 131.98, 130.14, 129.97, 129.67, 129.30, 128.83, 128.58, 128.23, 128.11, 128.03, 127.22, 126.99, 67.98, 66.95, 64.77, 63.46, 63.41, 55.62, 51.84, 38.70; MS (ES^+): m/z 538 (MH^+).

(S,S,S,R)-1-(2-(N-*t*-Butoxycarbonylasparaginy)amino-2-benzyl-1-hydroxypropyl)-N-methyl-N-benzylaminobenzoylimide (AQ174). ^1H NMR: δ 1.46 (s, 9), 2.53 (dd, 16.3 and 4.81, 1), 2.86–3.05 (m, 4), 3.31–3.38 (m, 1) 3.53 (s, 3), 3.94–3.99 (m, 1), 4.26 (d, 5.1, 1), 4.38 (d, 9.9, 1), 4.43–4.56 (m, 1), 5.29–5.32 (m, 1), 5.56–5.58 (m, 1), 5.90–5.93 (m, 1), 5.97 (d, 13.5, 1), 6.85 (d, 8.1, 2), 7.23–7.40 (m, 12), 7.87–7.89 (m, 2); ^{13}C NMR: δ 173.25, 171.24, 169.51, 155.63, 137.75, 132.22, 132.16, 130.44, 130.24, 129.58, 129.51, 129.18, 128.76, 128.69, 128.03, 127.99, 127.49, 127.39, 126.81, 80.58, 67.97, 65.40, 60.34, 53.46, 52.12, 37.94, 36.68, 28.33; MS (AP^+): m/z 618 (MH^+).

(S,S,R)-1-(2-(N-*t*-Butoxycarbonyl)amino-2-(2-amino-benzyl)-1-hydroxypropyl)-N-methyl-N-benzylaminocyclohexylcarbonylimide (AQ175). ^1H NMR (300 MHz): δ 1.22–1.34 (m, 4), 1.43 (s, 9), 1.64–1.86 (m, 6), 2.00–2.04 (m, 1), 2.84 (d, 12.9, 1), 2.95–2.98 (m, 2), 3.04–3.12 (m, 1) 3.38 (s, 3), 3.52 (bs, 3), 3.99 (d, 12.9, 1) 4.37 (d, 10.2, 1), 5.28 (d, 9.9, 1), 5.78 (d, 12.9, 1), 5.93 (bs, 1), 6.14 (d, 7.5, 1), 6.59 (d, 6.3, 1), 6.94–6.99 (m, 1), 7.26–7.43 (m, 6); ^{13}C NMR (75.5 MHz): δ 178.75, 155.77, 146.98, 138.59, 130.34, 130.04, 129.89, 128.72, 128.45, 126.76, 121.67, 117.74, 116.14, 79.67, 67.34, 64.70, 62.81, 55.15, 51.73, 45.84, 38.83, 30.49, 30.33, 28.36, 26.28, 26.24, 26.17; MS (AP^+): m/z 525 (MH^+).

(S,S,S)-1-(2-(N-*t*-Butoxycarbonyl)-amino-2-(2-amino-benzyl)-1-hydroxypropyl)-N-methyl-N-benzylaminocyclohexylcarbonylimide (AQ176). ^2H NMR: δ 1.19–1.38 (m, 4), 1.42 (s, 9), 1.45–1.85 (m, 6), 1.95–2.05 (m, 1), 2.88–2.94 (m, 3), 3.36 (s, 3), 3.41–3.49 (m, 1), 3.69–3.72 (m, 3), 4.04 (d, 10.2, 1), 4.80 (d, 12.3, 1), 4.96 (d, 9.9, 1), 5.05 (d, 12.3, 1), 6.67–6.71 (m, 3), 7.09–7.30 (m, 8); ^{13}C NMR (75.5 MHz): δ 179.10, 155.71, 146.81, 137.82, 130.20, 129.58, 129.27, 128.45, 126.47, 122.39, 118.99, 116.41, 79.42, 69.05, 68.77, 66.32, 54.81, 48.30, 45.81, 38.61, 30.49, 30.32, 28.36, 26.38, 26.22, 26.14; MS (AP^+): m/z 525 (MH^+).

Protease expression and purification

Recombinant HIV-1 PR, HIV-2 PR, and SIV PR were expressed in *Escherichia coli* strain X90 as described previously.^{29–31} Recombinant HIV-2 PR and all mutant HIV-2 PRs were expressed in strain X90 using the pT2HIV2/115 vector.³⁰ The enzymes were purified to homogeneity as described.^{31,32} Concentrations of active

HIV-1 and HIV-2 PRs were determined by active site titration using the peptidomimetic inhibitor U-85548 (a gift of Dr A. Tomasselli, Upjohn), Val-Ser-Gln-Asn-Leu-y-[CH(OH)CH₂]-Val-Ile-Val.³³

In vitro assays of HIV-1 PR inhibitors

HIV-1 PR was assayed against the decapeptide Ala-Thr-Leu-Asn-Phe-↓Pro-Ile-Ser-Pro-Trp, which corresponds to the HIV-1 carboxy-terminal autoprocessing site.³⁴ The decapeptide was synthesized by conventional solid-state methods. Reactions were carried out as previously described.³⁵ Conversion of the decapeptide to the two pentapeptides was quantified by HPLC and compared with product standard curves. The IC₅₀ determinations were carried out at pH 5.5. Stock solutions of the inhibitors (5 µM–5 mM) were prepared in DMSO. Compounds were added to assay solutions and the final DMSO concentration adjusted to 5% (v/v). Baseline values were determined from enzymatic reactions containing 5% DMSO in the absence of inhibitor. HIV-1 PR was preincubated with the respective inhibitor for 1 min at 25 °C before initiating the reaction by adding the decapeptide substrate (250 µM final concentration). The extent of inhibition is independent of the incubation time, indicating reversible binding. In addition to the discontinuous HPLC assay, a fluorescent assay was utilized which monitored continuous peptide hydrolysis.^{36,37} HIV-1, HIV-2, and SIV PRs were assayed against the fluorescent substrate, ABZ-Thr-Ile-Nle-Phe(*p*-NO₂)-Gln-Arg-NH₂.

Stock solutions of both substrate (10 mM) and inhibitor (50–150 µM) were prepared in DMSO. Inhibitor was added to assay buffer (50 mM NaOAc, pH 5.5, 1 M NaCl, 1 mM DTT, 20% glycerol, 0.1% CHAPS) containing the respective enzyme, and preincubated for 1 min at 37 °C. The reaction was initiated by the addition of substrate (end concentration of 100 µM), and the final concentration of DMSO in the assay was 5% (v/v). Enzyme concentration ranged typically between 1 and 4 µg/mL per assay. Toxicity assays on the inhibitor were carried out as described previously using a stable cell line (CH-1) that produces all of the HIV-1 IIB2 proteins with the exception of envelope gp160.¹³

X-ray crystallographic structure determination

The 3-D structure of AQ148 in complex with its target HIV-1 PR was determined by the method of molecular replacement to a resolution of 2.5 Å and refined to a final *R* factor of 18.5%. Crystals of AQ148 and HIV-1 Q7K protease were grown from 1.0 M NaCl, 20 mM NaAc pH 5.4, 1.0 mM EDTA, and 1.0 mM DTT.³⁸ Diffraction intensities were measured using Cu-K_α radiation from a Rigaku generator at 30 mA and 40 kV and a Siemen's X-1000 position sensitive area detector from a single crystal with orthorhombic plate morphology and dimensions of 100 × 50 × 20 µm. Data were reduced and scaled in space group *P*2₁2₁2₁, *a* = 53.07, *b* = 60.95, *c* = 63.24 Å, using the Siemen's software to give an overall *R*_{sym} of 8.1% for 14,215

Table 3. Statistics of crystallographic data collection and structure refinement

	Resolution (Å)				
	4.3–∞	3.4–4.3	3.0–3.4	2.7–3.0	2.5–2.7
Crystallographic data					
<i>R</i> _{sym} (<i>I</i>) (%) ^a	8.0	6.2	8.5	13.8	15.1
Ave. <i>I</i> /sig(<i>I</i>)	53.1	28.6	14.8	9.1	6.2
No. of unique reflections, possible	1668	1589	1611	1607	1283
No. of reflections, collected	1640	1487	1489	1464	784
No. of observations, total	5143	3136	2609	2320	1005
Completeness of data (%)	98.3	93.6	92.4	91.1	61.1
Redundancy	3.1	2.1	1.7	1.6	1.3
<i>R</i> _{cryst} of refined structure (%) ^b	(7.0–4.3 Å) 15.6		16.3	23.3	25.9
	Bond lengths		Bond angles	Dihedral angles	Improper angles
RMS deviations from ideality in final model	0.021 Å		3.50°	30.1°	16.5°

$$^a R_{\text{sym}} = \left\{ \frac{\sum_{hkl} \sum_{i=1}^N (I_{\text{avg}} - I_i)^2}{\sum_{hkl} \sum_{i=1}^N (I_i)^2} \right\}^{1/2}$$

$$^b R_{\text{cryst}} = \frac{\sum (|F_o| - |F_c|)}{\sum |F_o|}$$

observations of 6594 unique reflections between 32 and 2.5 Å with an overall completeness of 87%. The crystallographic data are summarized in Table 3. Molecular replacement proceeded with a probe model of HIV-1 Q7K protease determined in our laboratory³⁸ with the ligands and waters removed, using the program X-PLOR.³⁹ The initial *R* factor for all data between 7.0 and 2.5 Å was 38.7%. Rigid body minimization reduced the *R* factor to 34.3% and least-squares positional refinement gave an *R* factor of 22.6%. At this point, a difference density map calculated using terms $(F_o - F_c)/\alpha_{\text{calc}}$ clearly defined the atomic positions of AQ148 and an associated water molecule in the active site.

Atomic coordinates for AQ148 modeled in the active site of the 8HVP HIV-1 PR structure were used to derive restraint parameters for further modeling and refinement using the program QUANTA (Polygen) with the CHARMM force field. The only obstacle to development of the parameters was encountered when defining the imide nitrogen. QUANTA uses the CHARMM force field and atom types which does not allow for this type of an atom. A compromise was reached by protonating the nitrogen. Although this imide nitrogen is near a well-ordered water molecule it is not directly involved with inhibitor/protein interactions and the final refined atomic position of the nitrogen atom and the relative positions of neighboring bonded atoms should not be affected by the protonation state of the modeled compound.

The $F_o - F_c$ electron density map was used to position the AQ148 model in the active site of HIV-1 PR. The hydroxyl group was centered in the electron density between the active site aspartic acid carboxylates and the four hydrophobic substituents were positioned using the allowed dihedral rotations. Least-squares positional refinement, simulated annealing refinement, hand rebuilding and inclusion of eight structural water molecules resulted in a final *R* factor of 18% for all data between 7.0 and 2.5 Å.

Acknowledgments

This research was supported by NIH grant GM39552. FM is supported by a fellowship from the American Foundation of AIDS Research. The atomic coordinates for the refined model will be deposited with the Protein Data Bank.

References

1. Popovic, M.; Sarngadharan, M. G.; Read, E.; Gallo, R. C. *Science* **1984**, *224*, 497.
2. Kramer, R. A.; Schaber, M. D.; Skalka, A. M.; Ganguly, K.; Wong-Staal, F.; Reddy, E. P. *Science* **1986**, *231*, 1580.
3. Darke, P. L.; Nutt, R. F.; Brady, S. F.; Garsky, V. M.; Ciccarone, T. M.; Leu, C. T.; Lumma, P. K.; Freidinger, R. M.; Veber, D. F.; Sigal, I. S. *Biochem. Biophys. Res. Commun.* **1988**, *156*, 297.
4. Navia, M. A.; Fitzgerald, P. M.; McKeever, B. M.; Leu, C. T.; Heimbach, J. C.; Herber, W. K.; Sigal, I. S.; Darke, P. L.; Springer, J. P. *Nature (London)* **1989**, *337*, 615.
5. Schechter, I.; Berger, A. *Biochem. Biophys. Res. Comm.* **1967**, *27*, 157.
6. Dreyer, G. B.; Lambert, D. M.; Meek, T. D.; Carr, T. J.; Tomaszek, T. A., Jr.; Fernandez, A. V.; Bartus, H.; Caccia-villani, E.; Hassell, A. M.; Minnich, M.; *Biochemistry* **1992**, *31*, 6646.
7. Wlodawer, A.; Erickson, J. W. *Annu. Rev. Biochem.* **1993**, *62*, 543.
8. Grobelny, D.; Wondrak, E. M.; Galardy, R. E.; Oroszlan, S. *Biochem. Biophys. Res. Comm.* **1990**, *169*, 1111.
9. Lam, P. Y.; Jadhav, P. K.; Eyermann, C. J.; Hodge, C. N.; Ru, Y.; Bacheler, L. T.; Meek, J. L.; Otto, M. J.; Rayner, M. M.; Wong, Y. N.; *Science* **1994**, *263*, 380.
10. Tichniouin, M.; Sauleau, J.; Sauleau, A.; Lacroix, P. *Eur. J. Med. Chem.* **1982**, *117*, 265.
11. Colombo, M.; Farre, A. J.; Fort, M.; Martinez, L.; Rose, R.; Sagarra, R. *Meth. Find. Exptl. Clin. Pharmacol.* **1987**, *9*, 101.
12. Peisach, E.; Casebier, D.; Gallion, S. L.; Furth, P.; Petsko, G. A.; Hogan, J. C.; Ringe, D. *Science* **1995**, *269*, 66.
13. Babé, L. M.; Craik, C. S. *Antimicrob. Agents. Chemother.* **1994**, *38*, 2430.
14. Swain, A. L.; Miller, M. M.; Green, J.; Rich, D. H.; Schneider, J.; Kent, S. B.; Wlodawer, A. *Proc. Natl Acad. Sci. U.S.A.* **1990**, *87*, 8805.
15. Bernstein, F. C.; Koetzle, T. F.; Williams, G. J. B.; Meyer, E. F.; Brice, M. D.; Rodgers, J. R.; Kennard, O.; Shimanouchi, T.; Tasumi, M. *J. Mol. Biol.* **1977**, *112*, 535.
16. Thompson, W. J.; Fitzgerald, P. M.; Holloway, M. K.; Emini, E. A.; Darke, P. L.; McKeever, B. M.; Schleif, W. A.; Quintero, J. C.; Zugay, J. A.; Tucker, T. J.; *J. Med. Chem.* **1992**, *35*, 1685.
17. Graves, B. J.; Hatada, M. H.; Miller, J. K.; Graves, M. C.; Roy, S. *Structure and Function of the Aspartic Proteinase: Genetics, Structure and Mechanisms*; Graves, B. J.; Hatada, M. H.; Miller, J. K.; Graves, M. C.; Roy, S., Eds.; Plenum: New York, 1992; pp 455–460.
18. Abdel-Meguid, S. S.; Zhao, B.; Murthy, K. H.; Winborne, E.; Choi, J. K.; DesJarlais, R. L.; Minnich, M. D.; Culp, J. S.; Debouck, C.; Tomaszek, T. A. Jr. *Biochemistry* **1993**, *32*, 7972.
19. Bone, R.; Vacca, J. P.; Anderson, P. S.; Holloway, M. K. *J. Am. Chem. Soc.* **1991**, *113*, 9382.
20. Condra, J. H.; Schleif, W. A.; Blahy, O. M.; Gabryelski, L. J.; Graham, D. J.; Quintero, J. C.; Rhodes, A.; Robbins, H. L.; Roth, E.; Shivaprakash, M.; *Nature (London)* **1995**, *374*, 569.
21. Abdel-Meguid, S. S.; Metcalf, B. W.; Carr, T. J.; Demarsh, P.; DesJarlais, R. L.; Fisher, S.; Green, D. W.; Ivanoff, L.; Lambert, D. M.; Murthy, K. H. M.; Petteway, S. R. J.; Pitts, W. J.; Tomaszek, T. A.; Winborne, E.; Zhao, B.; Dreyer, G. B.; Meek, T. D. *Biochemistry* **1994**, *33*, 11671.
22. Jaskolski, M.; Tomasselli, A. G.; Sawyer, T. K.; Staples, D. G.; Heinrikson, R. L.; Schneider, J.; Kent, S. B.; Wlodawer, A. *Biochemistry* **1991**, *30*, 1600.
23. Hagler, A. T.; Stern, P. S.; Lifson, S.; Ariel, S. *J. Am. Chem. Soc.* **1979**, *101*, 813.

24. Ghosh, A. K.; Lee, H. Y.; Thompson, W. J.; Culberson, C.; Holloway, M. K.; McKee, S. P.; Munson, P. M.; Duong, T. T.; Smith, A. M.; Darke, P. L.; *J. Med. Chem.* **1994**, *37*, 1177.
25. Luly, J. R.; Dellaria, J. F.; Plattner, J. J.; Soderquist, J. L.; Yi, N. *J. Org. Chem.* **1987**, *52*, 1487.
26. Still, W. C.; Kahn, M.; Mitra, A. *J. Org. Chem.* **1978**, *43*, 2923.
27. Ohme, R.; Preuschof, H. *J. Prakt. Chem.* **1970**, *312*, 349.
28. Ghosh, A. K.; Duong, T. T.; McKee, S. P. *Tetrahedron Lett.* **1991**, *32*, 4251.
29. Rosé, J. R.; Babé, L. M.; Craik, C. S. *J. Virol.* **1995**, *69*, 2751.
30. Salto, R.; Babé, L. M.; Li, J.; Rosé, J. R.; Yu, Z.; Burlingame, A.; De Voss, J. J.; Sui, Z.; Ortiz de Montellano, P.; Craik, C. S. *J. Biol. Chem.* **1994**, *269*, 10691.
31. Rose, R. B.; Rosé, J. R.; Salto, R.; Craik, C. S.; Stroud, R. M. *Biochemistry* **1993**, *32*, 12498.
32. Rosé, J. R.; Salto, R.; C.S., C. *J. Biol. Chem.* **1993**, *268*, 11939.
33. Tomasselli, A. G.; Hui, J. O.; Sawyer, T. K.; Staples, D. J.; Bannow, C.; Reardon, I. M.; Howe, W. J.; DeCamp, D. L.; Craik, C. S.; Heinrichson, R. L. *J. Biol. Chem.* **1990**, *265*, 14675.
34. Pichuantes, S.; Babé, L. M.; Barr, P. J.; DeCamp, D. L.; Craik, C. S. *J. Biol. Chem.* **1990**, *265*, 13890.
35. DesJarlais, R. L.; Seibel, G. L.; Kuntz, I. D.; Ortiz de Montellano, P. R.; Furth, P. S.; Alvarez, J. C.; DeCamp, D. L.; Babé, L. M.; Craik, C. S. *Proc. Natl Acad. Sci. U.S.A.* **1990**, *87*, 6644.
36. Matayoshi, E. D.; Wang, G. T.; Krafft, G. A.; Erickson, J. *Science* **1990**, *247*, 954.
37. Toth, M. V.; Marshall, G. R. *Int. J. Pept. Protein Res.* **1990**, *36*, 544.
38. Rutenber, E.; Fauman, E. B.; Keenan, R. J.; Fong, S.; Furth, P. S.; Ortiz de Montellano, P. R.; Meng, E.; Kuntz, I. D.; DeCamp, D. L.; Salto, R.; *J. Biol. Chem.* **1993**, *268*, 15343.
39. Brunger, A. T. *J. Mol. Biol.* **1988**, *203*, 803.

(Received in U.S.A. 25 October 1995)